

Quantum Opacity, the RHIC HBT Puzzle, and the Chiral Phase Transition

John G. Cramer, Gerald A. Miller, Jackson M. S. Wu and Jin-Hee Yoon*

*Department of Physics, University of Washington
Seattle, WA 98195-1560*

(Dated: October 26, 2018)

We present a relativistic quantum mechanical treatment of opacity and refractive effects that allows reproduction of observables measured in two-pion (HBT) interferometry and pion spectra at RHIC. The inferred emission duration is substantial. The results are consistent with the emission of pions from a system that has a restored chiral symmetry.

PACS numbers: 25.75.-q

The space-time structure of the “fireball” produced in the collision between two heavy ions moving relativistically is studied by measuring the two-particle momentum correlations between pairs of identical particles. The quantum statistical effects of symmetrization cause an enhancement of the two-boson coincidence rate at small momentum differences that can be related to the space-time size of the particle source. This method, called HBT interferometry, has been applied extensively in recent experiments at the Relativistic Heavy Ion Collider (RHIC) by the STAR and PHENIX collaborations [1].

The invariant ratio of the cross section for the production of two pions of momenta $\mathbf{p}_1, \mathbf{p}_2$ to the product of single particle production cross sections is analyzed as the correlation function $C(\mathbf{p}_1, \mathbf{p}_2)$. We define $\mathbf{q} = \mathbf{p}_1 - \mathbf{p}_2$ and $\mathbf{K} = (\mathbf{p}_1 + \mathbf{p}_2)/2$, with \mathbf{K}_T as the component perpendicular to the beam direction. (We focus on mid-rapidity data, where $\mathbf{K} = \mathbf{K}_T$.) The correlation function is parameterized for small \mathbf{q} as $C(\mathbf{q}, \mathbf{K}) \approx 1 + \lambda(1 - R_o^2 q_o^2 - R_s^2 q_s^2 - R_l^2 q_l^2)$, where o, s, l represent directions parallel to \mathbf{K}_T , perpendicular to \mathbf{K}_T and the beam direction, and parallel to the beam direction[2]. Early [3] and recent [1] hydrodynamic calculations predicted that a fireball evolving through a quark-gluon-hadronic phase transitions would emit pions over a long time period, causing a large ratio R_o/R_s . The puzzling experimental result that $R_o/R_s \approx 1$ [4] is part of what has been called “the RHIC HBT puzzle” [5].

Data shows the medium produced by 200 GeV Au+Au collisions to be very dense. Consequently, pions should emerge from an opaque source[6]. Analyticity tells us that opacity implies accompanying refractive effects. Our purpose here is to derive and apply a relativistic quantum-mechanical treatment of opacity and refractive effects that simultaneously reproduces the values of R_o, R_s, R_l and the pion spectrum for central RHIC Au+Au collisions[7, 8].

The experimental observables depend on an emission function, the Wigner transform of the density matrix for the currents that emit pions. This emission function has often been modelled (see review [9]), as a function S_0 having the form of a hydrodynamic source parameter-

ization with approximately boost-invariant longitudinal dynamics:

$$S_0(x, K) = S_0(\tau, \eta) B_\eta(\mathbf{b}, \mathbf{K}_T)/(2\pi)^3 \quad (1)$$

$$S_0(\tau, \eta) \equiv \frac{\cosh \eta}{\sqrt{2\pi(\Delta\tau)^2}} \exp \left[-\frac{(\tau - \tau_0)^2}{2(\Delta\tau)^2} - \frac{\eta^2}{2\Delta\eta^2} \right] \quad (2)$$

$$B_\eta(\mathbf{b}, \mathbf{K}_T) \equiv M_T \frac{1}{\exp(\frac{K \cdot u - \mu_\pi}{T}) - 1} \rho(b), \quad (3)$$

in which components of x^μ are expressed using the variables $\tau = \sqrt{t^2 - z^2}$, $\eta = \frac{1}{2} \log \frac{t+z}{t-z}$, $\mathbf{b} \equiv (x_1, x_2)$, and $K \cdot u = M_T \cosh \eta \cosh \eta_t(b) - K_T \sinh \eta_t(b) \cos \phi$, where ϕ is the angle between \mathbf{K}_T and \mathbf{b} , $M_T = \sqrt{K_T^2 + m_\pi^2}$, and μ_π is the pion chemical potential. The function $\rho(b)$ represents the cylindrically symmetric transverse source density. We use $\rho(b) = [1/(\exp((r - R_{WS})/a_{WS}) + 1)]^2$, reflecting superimposed nuclear densities. Eq. (1) represents the transverse flow rapidity using a linear radial profile of strength η_f : $\eta_t(b) = \eta_f \frac{b}{R_{WS}}$. Eq. (1) incorporates the finite lifetime and size of the source: pions are emitted for a duration controlled by the parameters $\Delta\tau$ and $\Delta\eta$. Using Eq. (1) is not sufficient to capture all of the physics. As the basis of the blast wave parameterization, it gives $\Delta\tau \approx 0$ and does not predict the magnitude of the pion spectrum[10].

The salient feature of the 200 GeV data is the high density of the produced matter, so we treat the effects of pion interactions with the dense medium. We adopt a single-channel approach that uses the interaction-distorted incoming wave $\Psi_{\mathbf{p}_1}^{(-)*}(x_1)$ in which[11]:

$$S(x, K) = \int d^4 K' S_0(x, K') \int \frac{d^4 x'}{(2\pi)^4} e^{-iK' \cdot x'} \quad (4)$$

$$\times \Psi_{\mathbf{p}_1}^{(-)}(x + x'/2) \Psi_{\mathbf{p}_2}^{(-)*}(x - x'/2).$$

One could imagine a generalization in which Ψ would have two or more components (corresponding *e.g.* to a ρ final state in addition to a pion final state). Our task here is to compute pion correlation functions, so that it is sufficient to use a single channel wave function. One obtains the single-pion emission function from Eq. (4) by using the same momentum (either \mathbf{p}_1 or \mathbf{p}_2) to compute the wave function $\Psi_{\mathbf{p}}^{(-)}$.

Using Eq. (4) requires evaluating an eight-dimensional integral, and modelling the interactions that determine $\Psi_{\mathbf{p}_1}^{(-)}$. We use symmetries to reduce the number of integrals and obtain a tractable treatment of the interactions. First, note that $\Psi_{\mathbf{p}}^{(-)}(x)$ is an energy-eigenfunction [11]: $\Psi_{\mathbf{p}}^{(-)}(x) = e^{-i\omega_p x^0} \Psi_{\mathbf{p}}^{(-)}(\mathbf{x})$. We assume that the matter formed in the central region of the collision is cylindrically symmetric with a very long axis, so that

$$\Psi_{\mathbf{p}_{1,2}}^{(-)}(\mathbf{x}) = e^{\mp i q_l z/2} \psi_{\mathbf{p}_{1,2}}^{(-)}(\mathbf{x}_\perp = \mathbf{b}), \quad (5)$$

$$\mathbf{p}_{1,2} = \mathbf{K} \pm \mathbf{q}_T/2 \pm \hat{\mathbf{z}} q_l/2,$$

with $\psi_{\mathbf{p}}^{(-)}(\mathbf{b})$ obtained by solving a two-dimensional Klein-Gordon equation

$$(-\nabla_\perp^2 + U(b)) \psi_{\mathbf{p}}^{(-)*}(\mathbf{b}) = p^2 \psi_{\mathbf{p}}^{(-)*}(\mathbf{b}). \quad (6)$$

The ‘‘optical potential’’ U is a complex, azimuthally-symmetric function depending on pion momentum and local density that represents the strength of the interaction between a pion and the medium. Within our formalism the influence of time-dependent effects in U introduced by the time-dependent source S_0 is incorporated in the energy dependence of the optical potential. However, we note that the pions-medium interaction time is restricted by S_0 .

At large values of K the solution of Eq. (6) reduces to well-known semi-classical (eikonal) expression, but our procedure is more general. For example at $K=0$ there is no distinction between the out and side directions, so $R_o=R_s$. This constraint is violated if the eikonal approximation to (6) is used. We use a partial wave expansion:

$$\psi_{\mathbf{p}}^{(-)*}(\mathbf{b}) = f_0(p, b) + 2 \sum_{m=1, \infty} f_m(p, b) (-i)^m \cos m\phi \quad (7)$$

to solve Eq.(6) exactly and maintain the constraint.

The optical potential accounts for situations in which the pion changes energy or disappears entirely due to its interactions with the dense medium. Suppose, *e.g.*, that the medium is a gas of pions. Then $\pi\pi$ scattering would be the origin of U . In the impulse approximation, the central optical potential would be $U_0 = -4\pi f \rho_0$, where f is the complex forward scattering amplitude and ρ_0 the central density. For low energy pion-pion interactions, $4\pi \text{Im}[f(p)] = p\sigma$, with $\sigma \approx 1$ mb. At a momentum $p = 1 \text{ fm}^{-1}$, using a pion density about ten times the baryon density of ordinary nuclear matter, $\text{Im}[U(0)] \approx -0.15 \text{ fm}^{-2}$, representing significant opacity. Furthermore, if two interacting pions each have less energy than half of the rho meson mass, the final state interactions would be strongly attractive.

We model the interaction U for a situation in which the medium is dense, but we have not otherwise specified its nature. Now we consider chiral symmetry, which gives a general form for the dispersion relation of low energy

pions in nuclear matter:

$$\omega^2 = v^2(\hat{p}^2 + m_\pi^2(T)). \quad (8)$$

Here $m_\pi(T)$ is the π screening mass, v is the so-called π velocity, \hat{p} is the momentum operator, and the pole mass is $m_\pi(T)v$. Son and Stephanov[12] argued that v and the pion pole mass decreases at temperatures near the critical temperature, while the screening mass increases. Several papers have used specific low-order model calculations that challenge this result[13, 14]. Here we start with the general form (8) that appears in both Refs. [12, 13] and use data to determine the parameters. We first define an equivalent U by using $\omega^2 \equiv p^2 + m_\pi^2$, Eq. (8), and the Klein Gordon equation $\hat{p}^2 + U = p^2$, to obtain:

$$U = -(m_\pi^2 - v^2 m_\pi^2(T)) - (1 - v^2)\hat{p}^2. \quad (9)$$

For matter of finite size, Eq. (9) suggests a potential with terms constant and proportional to \hat{p}^2 . The latter has the form $w_2 p^2 - \nabla \cdot w_K \nabla$, where $w_{2,K}$ are complex constants. For the 200 GeV data, the results prefer a small value of w_K , so we take $w_K = 0$. The optical potential is therefore modelled as:

$$U_p(b) = -(w_0 + w_2 p^2)\rho(b), \quad (10)$$

with w_0 real (no opacity at $p=0$). The density profile $\rho(b)$ is that specified in $S_0(x, K)$. This simple form is sufficient to account for the data we study.

Eqs.(1,10) are the essence of our model. These may be compared with the Buda-Lund model, which is an efficient representation of the data[15] in which the temperature and fugacity are taken as position-dependent functions appearing in a Boltzmann distribution. The effects of our optical potential could provide an explanation of those deduced dependencies.

The use of Eqs. (5,1) in Eq. (4) gives

$$S(x, K) = \frac{1}{(2\pi)^2} \mathcal{S}_0(\tau, \eta) e^{iq^0 t - iq_l z} \int d^2 b' \tilde{B}_\eta(\mathbf{b}, \mathbf{b}') \times \psi_{\mathbf{p}_1}^{(-)}(\mathbf{b} + \mathbf{b}'/2) \psi_{\mathbf{p}_2}^{(-)*}(\mathbf{b} - \mathbf{b}'/2), \quad (11)$$

where $\tilde{B}_\eta(\mathbf{b}, \mathbf{b}') \equiv \int d^2 K'_T B_\eta(\mathbf{b}, \mathbf{K}'_T) \exp[-i\mathbf{K}'_T \cdot \mathbf{b}']$. The range of the variable \mathbf{b}' appearing in $\tilde{B}_\eta(\mathbf{b}, \mathbf{b}')$ is controlled by a size, $1/T$ that is much smaller than the source size. Thus it is reasonable to ignore the $\pm \mathbf{b}'/2$ appearing in (11). Maintaining the phases is important, so we use $\psi_{\mathbf{p}}^{(-)*}(\mathbf{b} \pm \mathbf{b}'/2) \equiv e^{-i\mathbf{p} \cdot (\mathbf{b} \pm \mathbf{b}'/2)} \chi_{\mathbf{p}}(\mathbf{b} \pm \mathbf{b}'/2) \rightarrow e^{-i\mathbf{p} \cdot (\mathbf{b} \pm \mathbf{b}'/2)} \chi_{\mathbf{p}}(\mathbf{b})$. This approximation is exact in several different limits: plane wave, short wavelength, long wave length, and taking $(R_{WS} T \rightarrow \infty)$.

We expand the exponentials in (11) involving q^0, q_l to 2nd order, expand the Bose-Einstein function in a series of Boltzmann functions of temperature $T_n = T/n$, and analytically evaluate integrals over τ and η to obtain:

$$C(\mathbf{q}, \mathbf{K}_T) = 1 - q_l^2 R_l^2 - q_0^2 \beta^2 \tilde{\Delta} \tau^2 + \frac{|\Phi_{12}|^2}{\Phi_{11} \Phi_{22}}, \quad (12)$$

$$\begin{aligned}\Phi_{ij} &= \sum_n \int d^2b f_0(\xi_n(b)) \psi_{\mathbf{p}_i}^{(-)}(\mathbf{b}) \psi_{\mathbf{p}_j}^{(-)*}(\mathbf{b}) B_n(\mathbf{b}, \mathbf{K}_T) \\ B_n(\mathbf{b}, \mathbf{K}_T) &= \exp\left(\frac{\mu_\pi + K_T \sinh \eta_t(b) \cos \phi}{T_n}\right) M_T \rho(b) \\ R_l^2 &= \frac{(3\Delta\tau^2 + \tau_0^2) F_1(K)}{F_0(K)} \\ \widetilde{\Delta\tau}^2 &= (3\Delta\tau^2 + \tau_0^2) \frac{F_3(K_T)}{F_0(K_T)} - \left| \frac{(\tau_0^2 + \Delta\tau^2) F_2(K_T)}{\tau_0 F_0(K_T)} \right|^2 \\ F_m(K) &= \sum_n \int d^2b B_n(\mathbf{b}, \mathbf{K}_T) f_m(\xi_n(b)) |\psi_{\mathbf{K}_T}^{(-)}(\mathbf{b})|^2\end{aligned}$$

where $\xi_n(b) = M_T \cosh \eta_t(b)/T_n + 1/\Delta\eta^2$, $f_1(\xi) \equiv 2K_0(\xi)/\xi + 4K_1(\xi)/\xi^2$, $f_0(\xi) \equiv 2K_1(\xi)$, $f_2(\xi) = K_0(\xi) + K_2(\xi)$, $f_3(\xi) = 2(K_1(\xi) + K_2(\xi)/\xi)$, and K_j are modified Bessel functions. The pion spectrum is given by:

$$\left\langle \frac{dN}{2\pi M_T dM_T dY} \right\rangle_{|Y| < 0.5} = \frac{\tau_0}{8\pi^3} e^{\frac{1}{\Delta\eta}} F_0(\mathbf{K}_T). \quad (13)$$

The angular integrals are performed analytically Eq. (7). The transverse HBT radii are $R_i(K_T) = \sqrt{1 - C(\Delta q_i, K_T)/\Delta q_i}$, with $i = o, s$ and $\Delta q_i \approx K_T/40$.

The values of the parameters $T, \eta_f, \Delta\tau, R_{WS}, a_{WS}, w_{0,2}, \tau_0, \Delta\eta$ and μ_π are varied to reproduce the STAR 200 GeV data for R_o, R_s, R_l [7] and the magnitude and shape of the pion spectrum [8]. The resulting parameters are displayed in Table I, with the variances that produce a χ^2 increase of one unit. The agreement of the curves with STAR HBT radii [7] in Fig. 1 and with the STAR pion spectrum [8] in Fig. 2 is quite good, giving a $\chi^2 \approx 3.7$ per data point and 5.6 per degree of freedom.

We need to assess and interpret the values of our parameters. The temperature ($T=173$ MeV) is comparable to the T_c expected for a chiral phase transition (≈ 160 MeV). The flow rapidity ($\eta_f=1.31$) corresponds to a maximum flow velocity of 0.85 c, which is not unreasonable. The source size is large ($R_{WS}=11.7$ fm), 4.4 fm larger than a gold nucleus ($R=7.3$ fm). If the system requires an expansion time $\tau_0 = 8.22$ fm/c to expand by this amount, the average expansion velocity would be about 0.5 c, which is reasonable. The emission duration ($\Delta\tau=2.9$ fm/c) is comfortably smaller than τ_0 . The longitudinal width ($\Delta\eta=1.063$) is smaller than expected, but is large enough that the system's axial length ($\sim 2\tau_0\Delta\eta \sim 17.5$ fm) is sufficient for the approximate validity of Eq. (5).

We assess the strength of U by examining it at $p \approx 1$ fm $^{-1}$. At the system center, the momentum-dependent term of U is $-(0.58+0.12i)$ fm $^{-2}$. To understand the imaginary part, which is comparable to our estimate given above (and consistent with the presence of high density matter), consider the equivalent classical mean free path: $p/|Im[U]| \approx 8$ fm $\ll 2R_{WS}$. Thus, the imaginary potential is large enough to restrict emission of pions from regions deep inside the medium. To understand the real part, note that the strength of the attraction is

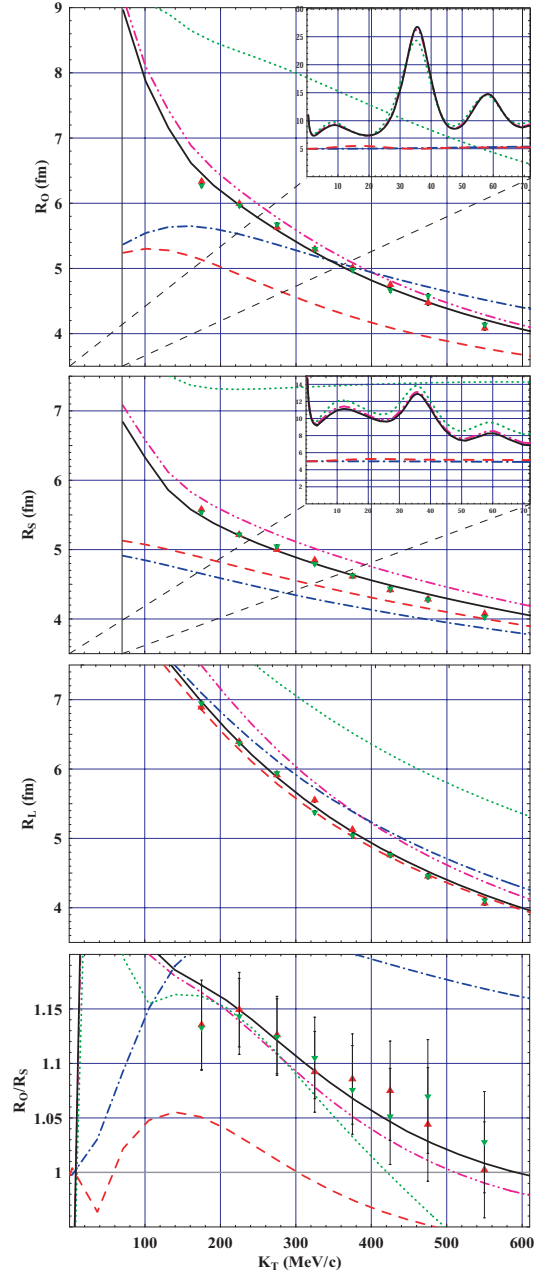


FIG. 1: (Color online) HBT Radii R_s, R_o, R_l and the ratio R_o/R_s ; Data [7]: ∇ (green) $\Rightarrow \pi^+\pi^+$; \triangle (red) $\Rightarrow \pi^-\pi^-$. Curves: solid (black) \Rightarrow full calculation; dotted (green) $\Rightarrow \eta_f = 0$ (no flow); dashed (red) $\Rightarrow \text{Re}[U]=0$ (no refraction); dot-dashed (blue) $\Rightarrow U=0$ (no potential), double-dot-dashed (magenta) \Rightarrow substituting Boltzmann for Bose-Einstein thermal distribution. Insets show predictions of low- K_T resonance behavior in R_o and R_s .

greater than $m_\pi^2 = 0.49$ fm $^{-2}$. Thus inside the medium, the pion acts as if it has no mass. This is why we assert that a chiral phase transition has occurred.

We further recall Eq. (9), and note that a momentum-dependent term of -0.58 fm $^{-2}$ corresponds $v = 0.65$. The

TABLE I: Parameters of the calculation with variances

$T(\text{MeV})$	η_f	$\Delta\tau(\text{fm}/c)$	$R_{WS}(\text{fm})$	$a_{WS}(\text{fm})$	$w_0(\text{fm}^{-2})$	w_2	$\tau_0(\text{fm}/c)$	$\Delta\eta$	$\mu_\pi(\text{MeV})$
173.2	1.314	2.852	11.728	0.725	0.137	$0.582 + i 0.121$	8.23	1.063	123.2
± 1.6	± 0.025	± 0.067	± 0.056	± 0.015	± 0.046	$\pm 0.014 \pm 0.002$	± 0.10	± 0.032	± 1.1

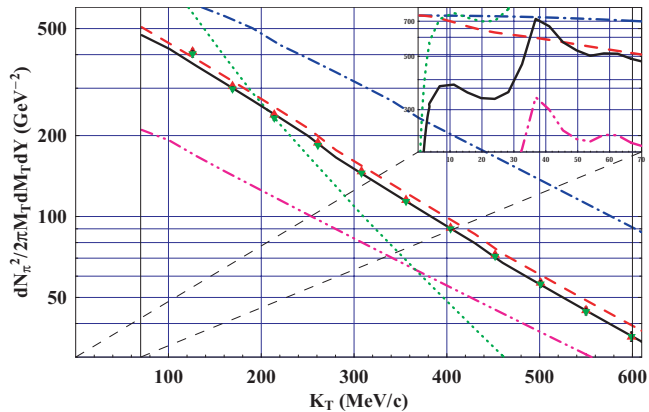


FIG. 2: (Color online) Pion momentum spectrum. Data [8]: ∇ (green) $\Rightarrow \pi^+$; \triangle (red) $\Rightarrow \pi^-$. Inset is low- K_T prediction.

momentum independent term of U (-14 fm^{-2}) corresponds to of $vm_\pi(T) = 0.6 \text{ fm}^{-1}$. These values are comparable to the estimates of [12], but not too far from the lowest value $v = 0.83$ of Ref. [14].

The chemical potential and Bose-Einstein distribution have modest effects on the radii but are very important for the normalization and slope of the pion spectrum.

Figs. 1, 2 show the importance of both the real and imaginary parts of the optical potential: omitting either drastically changes the predictions. The attractive real potential is the critical element needed to reproduce the K_T dependence of R_o and R_s .

We predict peaks in R_o and R_s at low momentum ($p \approx 15\text{--}65 \text{ MeV}/c$) and a rapid rise and peaking in the low-momentum spectrum. This is a pionic version of the Ramsauer effect, in which cross sections show peaks when the scattered wave is in phase with the incident plane wave. We confirm the computed existence of such peaks through analytic calculations for a purely real attractive square well potential. The PHOBOS detector (and perhaps the BRAHMS detector) at RHIC could, in principle, confront these low-momentum predictions of structure.

Our relativistic quantum-mechanical treatment of refractive and opacity effects on two-pion correlations and π spectra has surmounted a number of technical problems associated with previous semi-classical approximations, while achieving an excellent description of the 200 GeV STAR data. The results are consistent with the inter-

pretation that the dense medium has undergone a chiral phase transition. The definitive predictions of interesting momentum dependences at small momenta should be testable in present and future RHIC experiments.

This work is partially supported by the US-DOE grants DE-FG-02-97ER41014 and DE-FG-02-97ER41020. GAM thanks LBL, TJNAF and BNL for their hospitality during the course of this work. We thank J. Draper, S. Reddy and D. Son for useful discussions.

* Inha University, Republic of Korea.

- [1] P. F. Kolb and U. Heinz, nucl-th/0305084 (in *Quark Gluon Plasma 3*, Editors: R.C. Hwa and X.-N. Wang, World Scientific, Singapore)
- [2] S. Pratt, Phys. Rev. Lett. **53**, 1219 (1984). G. F. Bertsch *et al.*, Phys. Rev. **C37**, 1896 (1988).
- [3] D. H. Rischke and M. Gyulassy, Nucl. Phys. A **608**, 479 (1996)
- [4] C. Adler *et al.* [STAR Collaboration], Phys. Rev. Lett. **87**, 082301 (2001); K. Adcox *et al.* [PHENIX Collaboration], Phys. Rev. Lett. **88**, 192302 (2002); A. Enokizono [PHENIX Collaboration], Nucl. Phys. A **715**, 595 (2003).
- [5] U. W. Heinz and P. F. Kolb, hep-ph/0204061.
- [6] H. Heiselberg and A. P. Vischer, Eur. Phys. J. C **1**, 593 (1998); B. Tomasik and U. W. Heinz, Acta Phys. Slov. **49**, 251 (1999); D. Molnar and M. Gyulassy, Phys. Rev. Lett. **92**, 052301 (2004).
- [7] J. Adams, *et al.* [STAR Collaboration], Phys. Rev. C (submitted for publication, 2004);nucl-ex/0411036
- [8] J. Adams, *et al.* [STAR Collaboration], Phys. Rev. Lett. **92**, 112301 (2004).
- [9] U. A. Wiedemann and U. W. Heinz, Phys. Rept. **319**, 145 (1999).
- [10] F. Retière and M. A. Lisa, arXiv:nucl-th/0312024.
- [11] M. Gyulassy, S. K. Kauffmann and L. W. Wilson, Phys. Rev. C **20**, 2267 (1979).
- [12] D. T. Son and M. A. Stephanov, Phys. Rev. D **66**, 076011 (2002); D. T. Son and M. A. Stephanov, Phys. Rev. Lett. **88**, 202302 (2002)
- [13] D. Boyanovsky, H. J. de Vega and S. Y. Wang, Nucl. Phys. A **741**, 323 (2004).
- [14] C. Sasaki, arXiv:hep-ph/0404079.
- [15] M. Csanad, T. Csorgo, B. Lorstad and A. Ster, J. Phys. G **30**, S1079 (2004); T. Csorgo and B. Lorstad, Phys. Rev. C **54**, 1390 (1996); M. Csanad, T. Csorgo and B. Lorstad, Nucl. Phys. A **742**, 80 (2004).